Signal characteristics of charge-phase qubit detector with parametric energy conversion

V. I. Shnyrkov[a)]

B. I. Verkin Institute for Low-Temperature Physics and Engineering of the National Academy of Sciences of Ukraine, pr. Lenina 47, Kharkov 61103, Ukraine

A. A. Soroka

National Science Center "Kharkov Physicotechnical Institute," A. I. Akhiezer Institute of Theoretical Physics, ul. Akademicheskaya 1, Kharkov 61108, Ukraine

W. Krech

Friedrich Schiller University, Institute of Solid State Physics, Helmholtzweg 5, D-07743 Jena, Germany
(Submitted February 17, 2000)
Fiz. Nizk. Temp. **35**, 829–840 (August–September 2009)

The characteristics of a partially coherent quantum detector based on a charge-phase qubit, coupled with a classical ($\omega_T < k_B T/\hbar$) resonant circuit, are analyzed. It is shown that in an electromagnetic field signal characteristics with the maximum coefficient of conversion arise when the effective quantum inductance of the qubit assumes positive and negative values periodically with the frequency of low-frequency oscillations of the occupation probability of the energy levels (Rabi type) $\Omega_R \approx \omega_T$. The physical nature of parametric energy conversion (regeneration) in a qubit detector with a periodic change of the sign of the effective inductance and its possible application in quantum informatics for detecting weak signals is discussed. © *2009 American Institute of Physics*. [doi:10.1063/1.3224724]

I. INTRODUCTION

Experiments reliably demonstrate the presence of a superposition states in microscopic systems such as photons, electrons, atoms, and molecules, confirming the conceptual ideas at the heart of the theory of quantum mechanics. This is why micro-objects are being considered for constructing quantum bits (qubits) in the overwhelming majority of variants of quantum computers.[1] For a long time it was considered in experimental physics that a superposition for macroscopically distinguishable states of macroscopic objects is impossible to observe. In a Schrödinger clearly expressed in a thought experiment the existing contradiction between the superposition states of micro- and macro-objects,[2] which came to known as "Schrödinger's cat." In reality, quantum mechanics does not forbid the existence of a linear superposition of states of macroscopic objects, and the difficulty of creating and observing such states is due to their rapid decay, i.e. decoherence.[3–6] The transition from a purely superposition state into a mixed state (decoherence) occurs as a result of the coupling of a qubit with the large number of degrees of freedom of the environment. Investigations of the physical nature of the effects which result in decoherence in "artificial atoms"—superconducting qubits—and the suppression of these mechanisms is a topical problem in low-temperature physics and quantum informatics.[7–9]

There are several hopeful circumstances for building new, partially coherent, quantum devices and even, possibly, a quantum computer using superconducting qubits. In the first place, qubits based on nanosize Josephson contacts can be fabricated and replicated by modern technological methods with a high degree of integration. In the second place, the states of Josephson qubits, including entangled states, can be controlled selectively.[7–9] Only pulsed electric signals and weak magnetic fields are required to initialize a quantum processor. Finally, and perhaps most importantly, the states of Josephson qubits can be measured with high quantum efficiency, since in such a system a macroscopically large value of the magnetic moment ($\sim 10^{10}\mu_B \approx 10^{-13}$ J/T),[6] which can be viewed as a pseudospin, can participate in the coherent quantum dynamics. The development of the "hardware" for a quantum computer based on microscopic qubits is being held back precisely because there are no methods for rapidly measuring their state with high quantum efficiency.[1]

At the present time classical high-sensitivity detectors are used to study superconducting qubits (superpositions of macroscopic states, Rabi-oscillation type coherent dynamic effects, Landau–Zener interference, spin-echo) experimentally. These include single-electron transistors, squids, Josephson contacts, and linear and nonlinear oscillators.[6,8–18] The interaction of any classical detector with a quantum coherent system results in rapid collapse of the wave packet into one of the states, i.e. decoherence. Ordinarily, statistical measurements with so-called switchable detectors are used to study the dynamics within a certain time interval.[10,12–14] In this case, the detector, a squid (or Josephson contact), is in a superconducting state during the free evolution of a qubit and is switched into a resistive state during the measurement process. Next, a special impulse returns the qubit and the detector into the initial state, after which the measurement is repeated. After repeated measurements have been performed, mathematical analysis makes it possible to reconstruct the probability amplitude of the occupation probability of the levels at different moments in time and to determine the decay time of the low-frequency oscillations, which are similar to the Rabi effect in a two-level atom.

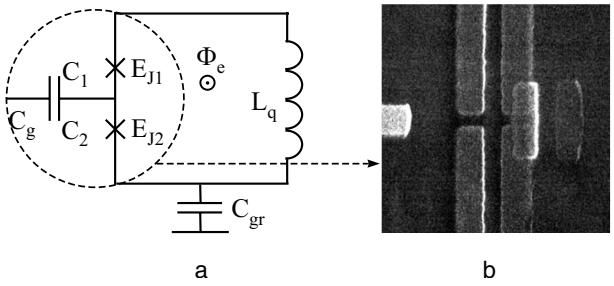

FIG. 1. Equivalent circuit of a charge-phase qubit with the parameters $C_g \approx 2\cdot 10^{-18}$ F, $C_{J1} \approx C_{J2} \approx 10^{-15}$ F, $C_{gr} \approx 0.5\cdot 10^{-12}$ F, $E_{J1}/h \approx 23$ GHz, $E_{J2}/h \approx 20$ GHz, and $L_q \approx 0.9\cdot 10^{-9}$ h (a). The image in an electron microscope (SEM) of the region of the "island" with two tunnel contacts $Al-Al_2O_3-Al$ and charge gate (b).

From the standpoint of experimental physics such methods can also be used in a quantum computer, but it is believed that quantum measurements of the states of qubits by the method of continuous indistinct measurements (weak continuous measurements—WCM) is prefereable.[16–24] The crux of this method is that during the measurement process a classical detector weakly perturbs the quantum object on which measurements are being performed, which results in "slow" decoherence of the state. Actually, this means that a classical detector is weakly coupled to the quantum object, which is the object of measurement, via a certain coefficient $k \ll 1$ and, obtaining a small part of the information about the object (weak measurements), has a weak "back effect" on the qubit in a wide frequency band.

A fundamentally new method of performing weak continuous measurements on quantum objects can be developed on the basis detectors using the nonlinear properties of a superposition of macroscopic states in flux or charge-phase qubits.[15,25–28] In this case a two-level quantum coherent system (qubit) will interact (form entangled states) with a partially coherent quantum detector in the course of the measurements. In principle a qubit detector, being an ideal parametric quantum transducer (an rf squid in a zero-hysteresis regime serves as a classical analog[29]), can have a minimal back effect on the object of measurement.

The objective of the present work is to investigate by the method of weak continuous measurements the signal characteristics of a charge-phase qubit[26–28] in a resonance microwave field (charge gate) and a weak rf field from a resonant circuit coupled with the qubit (phase gate).

II. MODEL OF A CHARGE-PHASE QUBIT

An artificial "atom"[9] based on a charge-phase qubit (Fig. 1) consists of a "single Cooper-pair-box" (SCPB), connected into a superconducting ring with inductance L_q, i.e. it is topologically similar to an rf squid[26–28] with an SCPB replacing the junction. A single-Cooper-pair box consists of two mesoscopic contacts with Josephson energies E_{J1} and E_{J2}, capacitances C_1 and C_2, and an island (granules) with a small volume placed between them. The value of the order parameter $\Delta(0)$ at the edges of the Josephson junctions and the number N of states, which is proportional to the volume of the island, determine the characteristic activation temperature of quasiparticle excitation $T^* = \Delta(0)/k_B \ln N$.[30] The voltage V_g of the charge gate, coupled with the island capacitance C_g, controls the magnitude of the polarization charge and the current circulating in the ring.

The Hamiltonian of the charge-phase qubit assumes its simplest form when the electrostatic energy of the SCPB is much greater than ($E_{CP} \gg E_J(\varphi)$) its effective Josephson energy. In this case the two "physical" base states of the qubit are coupled with zero or one Cooper pair, which has tunneled onto the island through the Josephson junctions. In the two-level approximation and limit of low inductance of the qubit circuit, the Hamiltonian in the basis of characteristic states (superposition states with respect to the initial physical states) has the form[28]

$$\hat{H}_q = \frac{1}{2}\Delta E(n_g,\varphi)\hat{\sigma}_z = \frac{1}{2}[E_J^2(\varphi) + D^2(n_g)]^{1/2}\hat{\sigma}_z \tag{1}$$

($\tilde{\sigma}_z$ is a Pauli matrix), where the effective Josephson energy

$$E_J(\varphi) = (E_{J1}^2 + E_{J2}^2 + 2E_{J1}E_{J2}\cos\varphi)^{1/2} \tag{2}$$

depends on the phase difference of the order parameter between both junctions $\varphi = \varphi_1 + \varphi_2$ (φ_1 and φ_2 are the phase differences between individual junctions), and the charge part of the Hamiltonian

$$D(n_g) = E_{CP}(1 - n_g) \tag{3}$$

is determined by $E_{CP} = (2e)^2/2C_\Sigma$ is the two-electron coulomb energy of the island with total capacitance $C_\Sigma = C_1 + C_2 + C_g$ and by the parameter $n_g = C_g V_g/e$ characterizing the proportional charge $en_g = C_g V_g$ induced on the island by the charge-gate voltage V_g. The geometric inductance L_g of the charge-gate qubit circuit is usually small in experiments, $L_q I_c/\Phi_0 \sim 10^{-2}$, so that the total magnetic flux Φ through the qubit circuit and the fixed external magnetic field Φ_e are related by the relation $\Phi \approx \Phi_e$, $\varphi \approx \varphi_e = 2\pi\Phi_e/\Phi_0$ and the Josephson energy of qubit is periodic in Φ with period Φ_0. Thus, according to Eq. (1) it is possible to control in a charge-phase qubit the effective Josephson energy $E_J(\varphi)$ by setting the external flux Φ_e and the effective charge energy $D(n_g)$ by setting the energy gap $\Delta E(n_g,\varphi)$ between the ground and excited levels of the qubit. An inhering feature of a charge-phase qubit (in contrast to an ordinary charge qubit), following from its topology, is the current circulating in the superconducting circuit of the qubit. The current operator for an isolated qubit corresponding to the Hamiltonian (1) has the form

$$\hat{I} = \frac{2e}{\hbar}\frac{\partial \hat{H}_q}{\partial \varphi} = I_q(n_g,\varphi)\hat{\sigma}_z, \quad I_q(n_g,\varphi) = \frac{e}{\hbar}\frac{E_{J1}E_{J2}\sin\varphi}{\Delta E(n_g,\varphi)}, \tag{4}$$

and therefore two basis states of a charge-phase qubit (ground and excited energy states) can be distinguished according to the superconducting currents $I_q(n_g,\varphi)$ circulating in opposite directions in the qubit circuit.

For arbitrary values of the ratio $E_J(\varphi)/E_{CP}$ the energy spectrum and the characteristic functions of the charge-phase qubit are given by the Bloch zones $E_n(n_g,\varphi)$ and the Bloch wave functions $|n_g,\varphi;n\rangle$ ($n = 1,2,\ldots$ is the zone index), which are the numerical solution of the Schrödinger equation with a Hamiltonian that includes all charge states and the

periodic Josephson energy.[26,27,31] The two lowest energy levels $E_n(n_g,\varphi)$ (with $n=0,1$) correspond to the basis of a charge-phase qubit in which the Hamiltonian has the form[26,27]

$$\hat{H}_q=\frac{1}{2}\Delta E(n_g,\varphi)\hat{\sigma}_z,\quad \Delta E=E_1(n_g,\varphi)-E_0(n_g,\varphi), \tag{5}$$

and the operator $\hat{I}=(2e/\hbar)\partial\hat{H}_q/\partial\varphi$.

The constant voltage V_{g0} controls the qubit detector via the charge gate, and the detector is excited by the electric component of the microwave field with frequency ν and amplitude V_r. The total voltage on the gate $V_g=V_{g0}+V_r\cos 2\pi\nu t$ polarizes the qubit island with charge C_gV_g. The quantum-dynamic response of the qubit is investigated by the standard, for microwave squids, method of signal detection[32,33] on the basis of the concept of weak continuous quantum measurements.[19–22] In principle, the signal of the charge-phase qubit can enter an amplitude or a phase detector. Analysis shows that the differences between the signal characteristics are not too great, so that we shall be concerned primarily with case of phase detection. In this scheme a qubit is weakly ($k^2\leqslant Q^{-1}$) coupled via the mutual inductance $M=k(L_qL_T)^{1/2}$ with a high-Q resonant circuit ($Q\gg 1$) with the characteristic frequency $\omega_T=(L_TC_T)^{1/2}$, which is a classical linear detector. A current from a high-resistance pump generator $I_P=I_{P0}\cos\Omega_P t$ is passed through this circuit; the amplitude of this current is practically independent of any changes of the impedance of the circuit. In the limit of small amplitudes I_{P0} the qubit impedance changes introduced into the circuit result in a small change of the amplitude V_T of the ac voltage $V=V_T\cos(\Omega_P t+\alpha_T)$ on the L_TC_T circuit and a shift α_T of its phase with respect to the phase of the pump current.

This method makes it possible to measure directly the quantum effective inductance of the qubit, characterizing the response of the qubit to a change of the external magnetic flux $d\langle\hat{I}\rangle/dt=L_J^{-1}d\Phi/dt$. For example, for adiabatic conditions and relatively low frequencies $\omega_T=\Omega_P\ll\Delta E(n_g,\varphi)$ and small pump amplitudes $\Phi_T=MQI_{P0}\ll\Phi_0$, moving along the energy state of a qubit $|n_g,\varphi;n\rangle$ the phase shift α_T can be represented in the form[18,34]

$$\tan\alpha_T(n_g,\varphi;n)=k^2Q\frac{L_qL_{Jn}^{-1}(n_g,\varphi)}{1+L_qL_{Jn}^{-1}(n_g,\varphi)}, \tag{6}$$

where the quantum effective inductance of a qubit characterizing the state $|n_g,\varphi;n\rangle$ is given by the expression[27]

$$L_{Jn}^{-1}(n_g,\varphi)=\frac{2\pi}{\Phi_0}\frac{\partial I_n(n_g,\varphi)}{\partial\varphi}=\left(\frac{2\pi}{\Phi_0}\right)^2\frac{\partial^2E_n(n_g,\varphi)}{\partial\varphi^2}. \tag{7}$$

As one can see from Eq. (7), the reciprocal of the effective inductance $L_{Jn}^{-1}(n_g,\varphi)$ is proportional to the local curvature of the energy level of a qubit $E_n(n_g,\varphi)$ with respect to φ. The sign and magnitude of $L_{Jn}^{-1}(n_g,\varphi)$ for two basis states of the qubit $n=0,1$ characterize the form of the corresponding energy bands $E_0(n_g,\varphi)$ and $E_1(n_g,\varphi)$. In the absence of a microwave field ($V_r=0$) the qubit is in the ground state and the experimentally measured function $\alpha_T(\varphi)$ makes it possible to reconstruct according to the relations (6) and (7) the "current-phase" dependence of a qubit

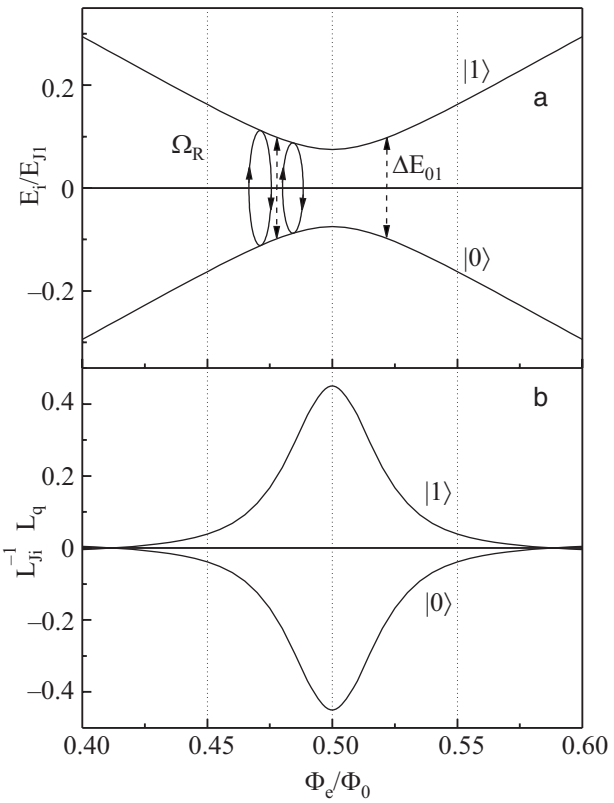

FIG. 2. Scheme of the dependences of the ground-state $|0\rangle$ and excited-state $|1\rangle$ energy levels of charge-phase qubit versus the external magnetic field. The arrows show Rabi-type oscillations with frequency Ω_R of the occupation probability of levels near exact resonance with an external microwave field, $\Delta E_{01}=h\nu$ (a). Curves of the effective quantum inductance in the ground and excited states versus the external magnetic flux Φ_e (b). It is evident that during part of the period of the low-frequency oscillations of the reactive parameter L_J^{-1} of the qubit assumes negative values. Computed parameters $L_q=0.9$ nh, $I_{c1}=50$ nA, $I_{c1}/I_{c2}=0.85$.

$$I_0(n_g,\varphi)=\frac{\Phi_0}{2\pi L_q}\int_0^{\varphi}\frac{\tan\alpha_T(\varphi')}{k^2Q-\tan\alpha_T(\varphi')}d\varphi'. \tag{8}$$

Figure 2a shows a diagram of the energy levels $E_0(1,\varphi)$ and $E_1(1,\varphi)$ of a charge-phase qubit with the Hamiltonian (1) for the two-level approximation; Fig. 2b shows the corresponding curvature of the functions $L_{J0}^{-1}(1,\varphi)$ and $L_{J1}^{-1}(1,\varphi)$ with a constant charge. The characteristic form of these dependences reflects the strong nonlinear dependence of the curvature of the energy levels $E_0(n_g,\varphi)$ and $E_1(n_g,\varphi)$ on the external flux φ. Moving along the level the qubit changes the effective inductance $\Delta L_T\sim -M^2L_J^{-1}(n_g,\varphi)$ of the circuit; according to (6), in the limit of small amplitudes of the rf generator the measured phase signal $\tan\alpha_T(n_g,\varphi;n)$ is determined by the local curvature of the level $L_{Jn}^{-1}(n_g,\varphi)$, and in the event that $L_J^{-1}L_q\ll 1$

$$\tan\alpha_T(n_g,\varphi;n)\approx k^2QL_qL_{Jn}^{-1}(n_g,\varphi).$$

In the simple two-level model (1) the energy bands possess the symmetry $E_1(n_g,\varphi)=-E_0(n_g,\varphi)$ and therefore their local curvature has the same magnitude and the opposite sign: $L_{J1}^{-1}(n_g,\varphi)=-L_{J0}^{-1}(n_g,\varphi)$ (Fig. 2b). However, the symmetry indicated above is a property of the two-level model; in general, $L_{J1}^{-1}(n_g,\varphi)\neq -L_{J0}^{-1}(n_g,\varphi)$ and the functions $L_{J1}^{-1}(n_g,\varphi)$, $L_{J0}^{-1}(n_g,\varphi)$ can differ in magnitude and sign.[26,27] Moreover, for a qubit interacting with a microwave field, even in the

two-level limit the local curvature of the quasienergy levels can deviate strongly from the indicated simple symmetry because the state depends on the amplitude of the microwave power.[35]

For resonance excitation of a two-level system by a microwave field the measured response is determined by the quantum-statistically averaged over the state of the qubit ($\hat{\rho} = \rho_{ij}|n_g,\varphi;i\rangle\langle n_g,\varphi;j|, i,j=0,1$) inductance $\langle L_J^{-1}(n_g,\varphi)\rangle$ introduced into the L_TC_T circuit:

$$\tan\alpha_T = k^2 Q L_q \langle L_J^{-1}(n_g,\varphi)\rangle / [1+\langle L_J^{-1}(n_g,\varphi)\rangle],$$

Since the inductances $L_{J0}^{-1}(n_g,\varphi)$ and $L_{J1}^{-1}(n_g,\varphi)$ of the ground and excited levels can differ in magnitude and sign, the change of the dependence $\tan\alpha_T(n_g,\varphi)$ with resonance single- or multiphoton excitation of a qubit relative to its form for a qubit in the ground state makes it possible to perform spectroscopy for the magnitude of the energy splitting $\Delta E(n_g,\varphi)$.[17,18] We note that in the experiments on Landau–Zener interferometry of a charge-phase qubit [in the charge limit $E_{CP} \gg E_J(\varphi)$] using the method of weak continuous measurements the phase signal is determined by the effective quantum capacitance averaged over the quantum state of the qubit $\langle C_{\text{eff}}(n_g,\varphi)\rangle$, where the capacitance in the nth charge state $C_{\text{eff}}(n_g,\varphi;n) \propto \partial^2 E_n(n_g,\varphi)/\partial n_g^2$ is proportional to the local curvature of the energy level $E_n(n_g,\varphi)$ with respect to the quasicharge n_g.

An important new effect was recently investigated theoretically[20,36] and experimentally[37]—paramagnetic energy exchange in a system consisting of a qubit coupled with an L_TC_T circuit. This effect arises when a qubit interacts with a microwave field as a result of the existence in it of coherent low-frequency oscillations (Rabi type) with frequency Ω_R, close to the frequency of the L_TC_T circuit, $\Omega_R \approx \omega_T$. The low-frequency oscillations of the occupation probability of the states $|n_g,\varphi;0\rangle$ and $|n_g,\varphi;1\rangle$ with frequency Ω_R are shown schematically in Fig. 2a. For the appearance of unusual electrodynamics in this system it is important that the reactive parameter of the "artificial atom" (7), changing in time with frequency Ω_R, can periodically assume negative values. In this case it is possible to observe changes not only of the imaginary part of the impedance of the L_TC_T circuit, owing to the effective inductance introduced from the qubit, but also changes of the real part of its impedance. Coherent oscillations of the effective inductance of a qubit with sign change result in the fact that the real part of the impedance, introduced into the L_TC_T circuit from the qubit, can become negative or positive, which corresponds to absorption or emission of energy by the "artificial atom." New quantum parametric detectors can be developed based on this effect. The characteristics of one such detector are examined below.

III. CHARGE-PHASE QUBIT AND EXPERIMENTAL PROCEDURE

A charge-phase qubit with dipole topology (Fig. 1) and $L_q \approx 0.9$ nh was fabricated using thin-film aluminum technology[17,18] with two tunneling contacts $Al-Al_2O_3-Al$ with area $S_{1,2} \approx 2.5\cdot 10^{-2}$ μm^2 and critical current density $j \approx 160$ A/cm^2. Optical measurements show that the areas of the contacts in this sample differ by 12–15%. Since the specific capacitance of such contacts is ~ 35 fF/μm^2, we obtain

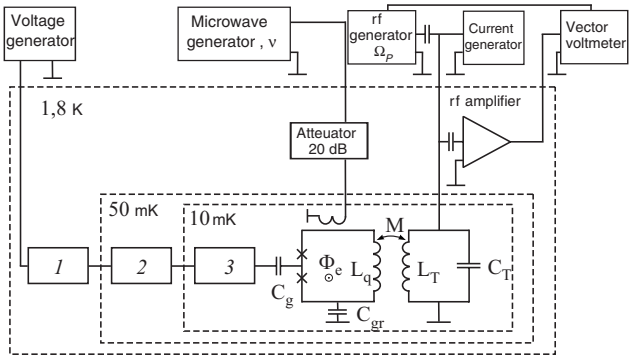

FIG. 3. Block diagram of the experimental investigations of the characteristics of a charge-phase qubit. The dashed lines enclose temperature regions of the dilution refrigerator and the elements located within them. The polarization charge on the island was produced from a voltage generator coupled with the charge gate C_g of the system of cooled filters. The qubit is enclosed in a lead screen (not shown in the figure), which for microwave frequencies is a cylindrical resonator. The microwave generator excited, through a coaxial cable with large damping and a cooled attenuator, a resonator at the frequency ν. Excitation of the L_TC_T circuit at the frequency Ω_R and detuning of the qubit with respect to the magnetic field were performed from rf and constant-current generators. The signal from the resonant circuit, coupled with the qubit by the mutual inductance $M=k\sqrt{L_TL_q}$, was amplified by a cooled amplifier and measured with a vector voltmeter. 1, 2, 3—powder (CuO) filter. 1) Voltage generator 2) Microwave generator, ν 3) rf generator, Ω_P 4) Current generator 5) Vector voltmeter 6) Attenuator 20 dB 7) rf amplifier

for the total capacitance of SCPB $C_\Sigma \approx C_1 + C_2 \approx 1.9\cdot 10^{-15}$ F for $C_{1,2} \gg C_g \approx 2\cdot 10^{-18}$ F. Hence we find that the maximum value of the coulomb energy neglecting the distributed capacitance is $E_{CP}=(2e)^2/2C_\Sigma \approx h\cdot 10$ GHz. An estimate obtained for the characteristic values of the Josephson energies of SCPB from optical measurements and measurements of the IVC of a control sample made in the same technology cycle as the qubit give $E_{J1}=I_{C1}\Phi_0/2\pi \approx h\cdot 20$ GHz and $E_{J2}=I_{C2}\Phi_0/2\pi \approx h\cdot 23$ GHz. We obtain from these values that in the absence of a microwave field the minimum value of the effective Josephson energy of a qubit at the point $\varphi=\pi$ is $E_{\min}(\varphi)=|E_{J1}-E_{J2}| \approx h\cdot 3$ GHz.

On the strength of the relations (4) and (7) the current circulating in the superconducting circuit of a qubit and the effective quantum inductance (impedance) are found to be periodic functions of the external flux Φ_e and the induced electric charge $q=C_gV_g$.[17] To measure small variations of the impedance the interferometer of the qubit L_q is coupled by the mutual inductance $M=k\sqrt{L_qL_T} \cong 0.434$ nh with a high-Q ($Q \cong 685$) resonant circuit $C_T \approx 185$ nF, $L_T \approx 168$ nh, excited by the current I_P of the pump generator at frequency Ω_P close to the resonance frequency of the circuit $\omega_T/2\pi \approx 28.55$ MHz (Fig. 3). The changes of the amplitude $V_T(n_g;\varphi)$ or phase $\alpha_T(n_g;\varphi)$, which were amplified by a cryogenic ($T_A \approx 1.7$ K) amplifier, of the oscillations of the resonant circuit can be regarded as output signal characteristics of the detector based on a charge-phase qubit. An advantage of such a scheme for recording impedance changes is that recording the signal at the pump frequency makes it possible to keep the $1/f$ type amplifier noise from reaching the output. In addition, the resonant circuit, being a linear detector, plays the role of a resonance transformer of impedances, matching a low-resistance qubit with the high input resistance of the amplifier.[32,33]

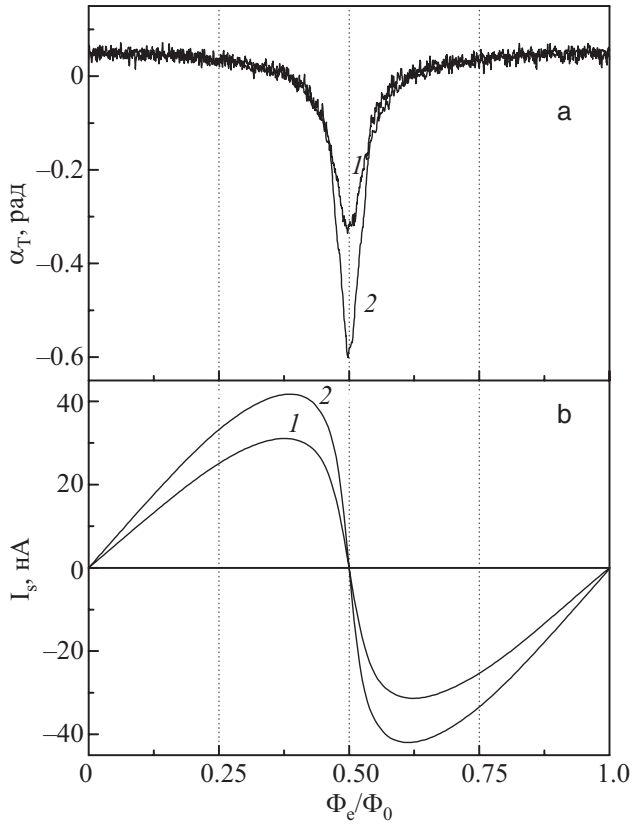

FIG. 4. Curves of the phase signal $\alpha_T(\Phi_e)$ on the resonant circuit coupled with a charge-phase qubit versus the external magnetic flux near $\Phi_e = \Phi_0/2$: 1—no filtering of the measuring channel; 2—with cooling to 10 mK with a powder filter in the chain of the resonant circuit (a). Curves of the amplitude of the superconducting current circulating in the qubit, constructed on the basis of the characteristics (1) and (2), versus the external flux (b).

The phase coherence of a qubit is destroyed by thermodynamic fluctuations of the current in the flux-gate circuit and the voltage in the charge-gate circtuit.[7,26] Three CuO-powder filters with total damping 120 dB at 5 GHz and >250 dB at 20 Ghz (Fig. 3) were installed to decrease the decoherence rate in a charge-gate circuit with $(C_g/C_1)^2 \sim 10^{-6}$. For the same purpose a magnetic bias was accomplished by means of a high-resistance (106 kΩ) circuit from the current generator through the coil of resonant circuit L_T with $\Phi_0/M \approx 4.76$ μA. To set the ac voltage on the charge gate $V_r \cos 2\pi\nu t$ and obtain Rabi-type oscillations the qubit was placed in the region of the maximum of the electric field of the superconducting resonator. Measurements of the spectral density of the low-frequency fluctuations of the magnetic flux at the location of the qubit show that the $1/f$ spectrum at the temperature of a ^{3}He–^{4}He dilution refrigerator $T = 10$ mK starts at the frequency 0.3–0.2 Hz. The analysis performed in Ref. 11, 38, and 39 shows that the nonquilibrium noise of the electric charge in dielectrics can start at much higher frequencies (10^2–10^3 Hz), and its spectral density depends on the losses in the material.

Another source of decoherence of a qubit in the continuous quantum measurement scheme is the cooled amplifier, whose back effect is difficult to estimate analytically. For this reason, in the present work measurements of the dependence of the effective inductance of the ground state of a qubit on the external magnetic flux Φ_e (Fig. 4) were performed for two different circuits. The measurements differ in that in one case the amplifier is directly connected to the circuit while in the second case an additional powder filter cooled to temperature 10 mK is inserted between them. As the dependences in displayed Fig. 4 show, the back effect of the amplifier (without a filter) results in strong smoothing of the local curvature of the energy level $\sim L_J^{-1}(n_g, \varphi; n)$ near $\Phi_e = \Phi_0/2$ and can be the main source of the increase in the effective noise temperature of the qubit and decoherence. The insertion of a filter cooled to 10 mK increases the signal amplitude $\alpha_T(n_g; \varphi)$, which is proportional to the local curvature of the ground-state energy level, by a factor of 1.7 (Fig. 4a). The ratio of the critical currents of the contacts, estimated from measurements performed with an additional cooled filter, equals $I_{c1}/I_{c2} \approx 0.8$, which agrees to within 10% with the optical measurements of the contact areas. It follows from these measurements that in the stationary case the superconducting current (8) circulating in this qubit sample (Fig. 4b) reaches its maximum value at the points $\Phi_e \approx \Phi_0(0.5 \pm 0.1)$, taking account of the fluctuations.

In the absence of a magnetic field the dependences of the local curvature of the ground-state energy on the external magnetic flux and charge can be used to develop magnetometers $E_J^2(\varphi) > D^2(n_g)$ and electrometers $E_J^2(\varphi) < D^2(n_g)$.[25–27] In this case the qubit-detector is a magnetometer or electrometer so that its output signal V_S is proportional to the variations $\delta\Phi$ of the magnetic flux or variations of the charge $\delta q = C_g \delta V_g$ on the qubit gates. Taking account of the output noise of the measuring circuit V_N, the voltage at the output can be represented in the form

$$V = V_N + \eta_\varphi \delta\Phi, \quad V = V_N + \eta_q \delta q. \tag{9}$$

Here $\eta_\varphi = \eta_0(dV_T/d\Phi_e)$ and $\eta_q = \eta_0(dV_T/dq)$ are the transformation coefficients in the magnetic field and charge, and $\eta_0 = (\Omega_P/k)(L_T/L_q)^{1/2}$ characterizes the measuring channel. In our case we have $\eta_0 \approx 6.5 \cdot 10^{10}$ s^{-1}. As noted in Refs. 26 and 37, the values of the derivatives $dV_T/d\Phi_e$ and dV_T/dq depend strongly on the local curvature of the energy levels of the qubit and the experimental conditions k, I_P, Q, $(\omega_T - \Omega_R)$ and can be optimized ($\eta_{\varphi,q} \geqslant \eta_0$ by adjusting the parameters. Neglecting the back effect of the qubit on the measured signal the signal/noise ratio can be characterized by the flux (or charge) equivalent to the noise $\Phi_N = V_N/\eta_\varphi$ (or $q_N = V_N/\eta_q$). In this case the main parameter of the qubit-detector—the energy sensitivity—can be expressed in terms of the spectral density of the quantities Φ_N, q_N in the band of the resonant circuit:

$$\delta\varepsilon_\varphi = \frac{\langle \Phi_N^2 \rangle}{2L_q B} = \frac{\langle V_N^2 \rangle}{2L\eta_\varphi^2 B}; \tag{10a}$$

$$\delta\varepsilon_q = \frac{\langle q_N^2 \rangle}{2(C_{J1} + C_{J2})B} = \frac{\langle V_N^2 \rangle}{2\eta_q^2 (C_{J1} + C_{J2})B}, \tag{10b}$$

where B is the output band, which is determined by the measuring time. Since the rf amplifier can have a considerable fluctuation effect on the resonant circuit, to estimate the noise contribution the temperature T_T of the circuit can be replaced by the effective temperature $T_{T*} = T_T + Q\omega_T L_T T_A / R_A$, which is the quantity to be minimized (see Fig. 4). In the case where the temperature T_A is low and the

amplifier resistances R_A are high the characteristic sensitivity of the qubit-detector will improve with increasing $\eta_{\varphi,q}$ and for large transformation coefficients it will be determined by the inhering noise of the qubit. An increase of the transformation coefficients of parametric detectors in the regime $k^2Q\beta_L > 1$ has been analyzed in detail in Ref. 27 and 40 and realized in Ref. 29 and 33. A periodic variation of the occupation of the levels (sign of the effective quantum inductance) of a charge-phase qubit with multiphoton pumping results in parametric transformation of the energy due to the appearance of "emission" and "absorption" effects[20,37] in a two-level quantum system. This effect, called in classical systems "nondegenerate single-frequency parametric regeneration," can be used to increase the transformation coefficients and to develop detectors with quantum-limited sensitivity (Quantum Limited Detector).

IV. CHARACTERISTICS OF A CHARGE-PHASE QUBIT IN AN ELECTROMAGNETIC FIELD

We now shall examine the amplitude and phase signal characteristics of a detector based on a charge-phase qubit placed in a resonance electromagnetic field. The frequency Ω_R of the coherent oscillations of the occupation probability between the ground $\tilde{E}_0(n_g,\varphi)$ and excited $\tilde{E}_1(n_g,\varphi)$ quasilevels depends on the amplitude V_r and the detuning of the frequency ν of the microwave field relative to the resonance frequency of the qubit $f_{10}=[\tilde{E}_1(n_g,\varphi)-\tilde{E}_0(n_g,\varphi)]/h$. An increase of the amplitude of the magnetic flux from the circuit $Q_T \sin \Omega_P t = MQI_P \sin \Omega_P t$ leads to the obvious effects of averaging of the local curvature (7) of the qubit levels,[17,26,27,41] so that in the present work the experimental investigations were performed in the limit of weak ($I_PQM \leqslant 3\cdot 10^{-4}\Phi_0$) rf generator currents. The generator frequency Ω_P was chosen to be equal to the resonance frequency of the circuit $\Omega_P \cong \omega_T/2\pi \approx 28.55$ MHz. It is easily shown that in this case, for small changes of the frequency $\omega_T(n_g,\varphi)$ of the parametric circuit the phase channel $\alpha_T(n_g,\varphi)$ of signal detection has the maximum curvature of transformation, and the change of the oscillation amplitude $V_T(n_g,\varphi)$ is practically proportional to the variations of the Q factor. Since the impedance introduced into the resonant circuit is proportional to the small parameter $k^2L_qI_q^2$, we have $\omega_T(n_g,\varphi)\cong\omega_T$ and the scheme shown in Fig. 3 is required in order to detect small phase changes in the oscillations of the circuit.

It follows from the spectroscopy of the resonance energy absorption lines of a charge-phase qubit with low the microwave field amplitude that the maximum response is observed at frequencies ν equal to 4.4, 8, and 17.5 GHz. If the frequency ν of the microwave field and the value of the constant voltage V_{g0} on the charge gate are fixed, then the resonance condition for the excitation of the qubit can be obtained by changing Φ_e as a result of the dependence of the effective Josephson energy of the qubit (2) on the external magnetic field. For small amplitudes V_r the characteristic frequencies satisfy the inequality $\Omega_R(V_r) < \omega_T$ and the low-frequency oscillations of the occupation numbers of the levels do not fall within the resonance band of the circuit. As the amplitude of the microwave field increases, the frequency of the coherent oscillations of the occupancies falls into the range $\Omega_R(V_r)\cong\omega_T\pm\Delta\omega_T$, which leads to the appearance of

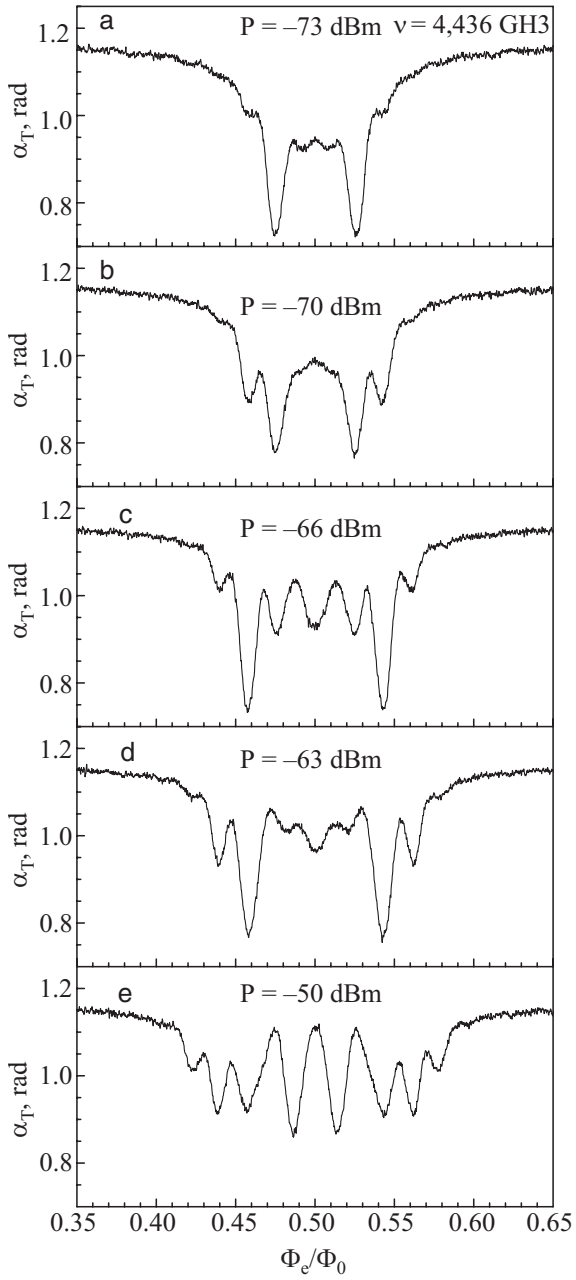

FIG. 5. Charge-phase qubit with $n_g \approx 1$ in a microwave resonance field with frequency 4.436 GHz. Family of curves of the phase signal characteristics $\alpha_T(\Phi_e)$ coupled with a qubit resonant circuit versus the external magnetic flux Φ_e. The parameter of the family is the output power of the microwave generator.

parametric energy transformation.[20,37] In such a process the basic condition for observing energy "emission" and "absorption" effects is a sufficiently high Q factor of the Rabi-type oscillations $\Omega_R/\Delta\Omega_R \gg 1$, where $\Delta\Omega_R$ is the frequency band of these oscillations.

Figure 5 displays measurements of the phases $\alpha_T(n_g \cong 1,\varphi)$ of the oscillations in the circuit as a function of the external magnetic field flux applied to the qubit in a microwave field with ν=4.436 GHz. The parameter of the family is the power of the microwave generator $P^{1/2} \propto V_r$. This figure shows that as V_r increases with sweeping of the external magnetic field quasiperiodic changes of the phase and frequency of the oscillations in the resonant circuit, which are associated with the impedance $Z(\omega)$ introduced by the qubit,

are observed. Analysis of the external magnetic flux dependence of the voltage on the resonant circuit $\Delta V_T(n_g \cong 1, \varphi) \propto -\mathrm{Re}\, Z(\omega)$ shows that three frequency ranges can be singled out: $\nu \gtrsim f_{01}(\varphi)$, $\nu \simeq f_{01}(\varphi)$, and $\nu \lesssim f_{01}(\varphi)$, for which the real part of the impedance introduced assumes the respective values $\mathrm{Re}\, Z(\omega) < 0$, $\mathrm{Re}\, Z(\omega) = 0$, and, $\mathrm{Re}\, Z(\omega) > 0$. In the region $h\nu > hf_{01}(\varphi)$ a "negative resistance" $\mathrm{Re}\, Z(\omega) < 0$ is introduced into the circuit and the circuit's Q factor increases[20,37] because energy is transferred from the qubit to the resonant circuit. When the resonance condition $h\nu = hf_{01}(\varphi)$ is satisfied, energy is conserved on average, and in the region $h\nu \leqslant hf_{01}(\varphi)$ energy is transformed in the opposite direction and the Q factor of the resonance ciruit decreases. The vertical arrow in Fig. 2a indicates exact resonance $h\nu = hf_{01}(\varphi)$, and the circular arrows to the right and left indicate the regions $h\nu > hf_{01}(\varphi)$ and $h\nu \leqslant hf_{01}(\varphi)$, respectively. Direct measurements showed that at the extremal points of the signal characersitics the magnitude of Q for a given qubit changes by approximately 15%. Analysis of the temperature dependences shows that to within the experimental error $\mathrm{Re}\, Z(\omega)$ is independent of the temperature of the refrigerator in the interval 10–40 mK. The amplitude $\mathrm{Re}\, Z(\omega)$ decreases by approximately a factor of two at $T = 150$ mK and $\mathrm{Re}\, Z(\omega) = 0$ at $T = 300$ mK.[37]

The effect of the quantum parametric energy transformation between the qubit and an LC circuit determines the form of the signal characteristics of the system $V_T(n_g \cong 1, \varphi)$ and $\alpha_T(n_g \cong 1, \varphi)$ in a resonance microwave field. The deviation of the positions of the extremal points of the signal characteristic along the Φ_e axis from exact resonance, the maximum values of impedance max $\mathrm{Re}\, Z(\omega)$, and the transformation coefficients

$$\eta_V(\varphi) = \left| \frac{dV_T}{d\Phi_e} \right|_{n_g=\mathrm{const}}, \quad \eta_\alpha(\varphi) = \left| \frac{d\alpha_T}{d\Phi_e} \right|_{n_g=\mathrm{const}} \tag{11}$$

can be explained by the finite band of low-frequency oscillations Ω_R, which is determined by the influence of external noise and the internal mechanisms of decoherence.

As the amplitude of the microwave field increases, a quasiperiodic dependence of the signal characteristics (Fig. 5c–5e) on the external magnetic flux is observed. The period of this dependence ($\Delta\Phi_e \approx 0.01 - 0.02\Phi_0$) is related with the satisfaction at certain values of φ of the resonance conditions for multiphoton excitations with increasing effective Josephson energy $E_J(\varphi)$. For the dependence in Fig. 5e the maximum range of the signal characteristic and the maximum of the transformation coefficient are observed in the region ($\varphi \cong \pi$) where for the stationary Hamiltonian (1) the current circulating in the circuit assumes its minimum value. This effect, which arises as the amplitude V_r increases, indicates the complicated behavior of the average values of the quasienergy levels of a charge-phase qubit in a microwave field[35] and could be helpful for performing spectroscopy of the states of a qubit in a microwave field with large amplitude.

We shall now examine the signal characteristics in the region of a high-frequency resonance, observed at the frequency $\nu = 17.5$ GHz. Figure 6 shows the signal characteristics $\alpha_t(\varphi, n_g)$ of a detector based on a charge-phase qubit, which were obtained with constant power of the microwave

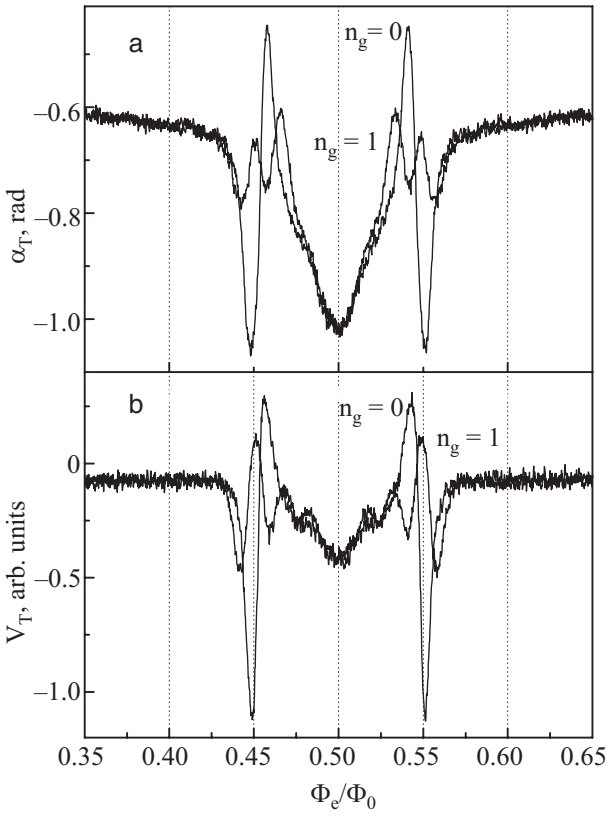

FIG. 6. Signal characteristics of the charge-phase qubit-detector in a microwave field with frequency 17.5 GHz at the constant power of the microwave generator $P = -65$ dBm. The phase signal in the resonant circuit for the values of the polarization charge $\alpha_T(\Phi_e, n_g = 1)$ and $\alpha_T(\Phi_e, n_g = 0)$ as a function of the external magnetic flux (a). The dependence of the change of the voltage on the resonant circuit $V_T(\Phi_e, n_g = 1)$ and $V_T(\Phi_e, n_g = 0)$ versus the magnetic flux. The family was obtained with the minimum detuning of the generator frequency from the resonance frequency of the circuit $\omega_T \cong \Omega_R$ and $MI_T \ll \Phi_0$ (b). 1) α_T, rad 2) V_T, arb. units

field $P = -65$ dBm, for two values of the voltage $C_g V_g / e = n_g \cong 1$ and $n_g \cong 0$ on the charge gate. It is evident that at the maximum value of the charge term $D(n_g = 0)$ the full range and the transformation coefficient $n_\alpha(\varphi)$ of the phase signal characteristics are appreciably greater than for $n_g \cong 1$. For an electrometer based on a qubit, just as for the transformation coefficients with respect to the magnetic flux, amplitude and phase transformation coefficients can be introduced for the electric charge:

$$\eta_V(n_g) = \left| \frac{dV_T}{dq_g} \right|_{\varphi=\mathrm{const}}; \quad \eta_\alpha(n_g) = \left| \frac{d\alpha_T}{dq_g} \right|_{\varphi=\mathrm{const}}. \tag{12}$$

The maximum difference between the phase signals shown in Fig. 7a $\alpha_T(\varphi, \Delta n_g = 1) = \alpha_T(\varphi, \Delta n_g = 0) - \alpha_T(\varphi, \Delta n_g = 1)$ characterizes the average ($\Delta n_g \cong 1$) value of the phase transformation coefficient with respect to the charge $\eta_\alpha(n_g)$ at the working point close to the optimal point with respect to the magnetic flux. The corresponding amplitude signals are presented in Fig. 7b.

Comparing the characteristics presented in Fig. 4 and Fig. 6a shows that the parametric transformation of energy increases $\eta_\alpha(\varphi)$ (and $\eta_V(\varphi)$ by a factor of approximately 5.4 for a qubit-based magnetometer. An even larger (by up to a factor of 8.3) increase of the transformation coefficients is

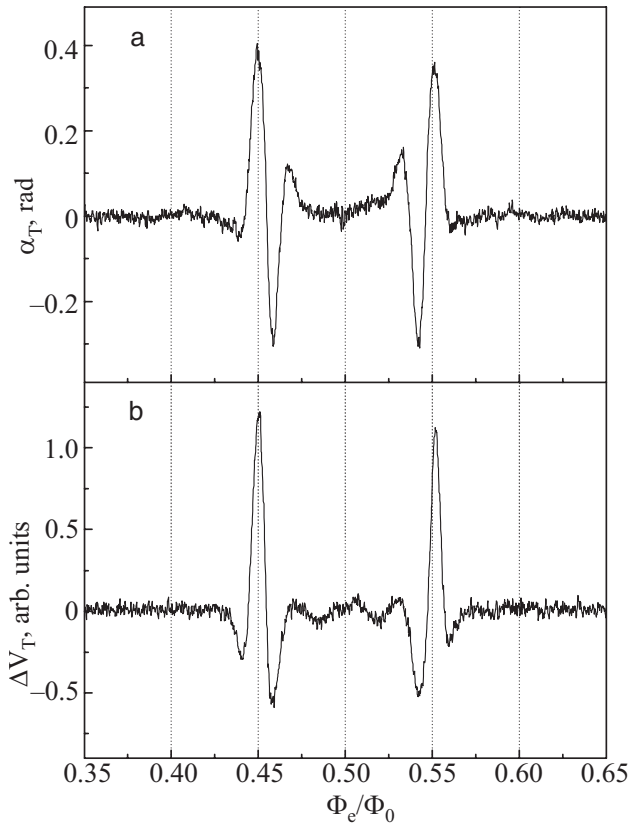

FIG. 7. Phase difference $\Delta\alpha_T(\Phi_e)=\alpha_T(\Phi_e,n_g=1)-\alpha_T(\Phi_e,n_g=0)$ (a) and amplitude difference $\Delta V_T(\Phi_e)=V_T(\Phi_e,n_g=1)-V_T(\Phi_e,n_g=0)$ (b) for the signal characteristics of qubit-detector which are shown in Fig. 6.

obtained in Ref. 37, where the inductance of a qubit is implemented in the form of a gradient meter to decrease the effect of the external $1/f$ noise flux.

It is evident from the structure of the Hamiltonian (1) and the characteristics obtained for a qubit-detector in an electromagnetic field that the transformation coefficients with respect to a weak signal (11) must depend not only on the magnetic flux but also on the choice of the working point with respect to the charge induced on the gate. Actually, maximum changes in the signal characteristics and hence large values of the transformation coefficients with respect to the charge are observed near $n_g \approx 0$. Figure 8 shows the change in the signal characteristic $\alpha_T(\varphi,n_g)$ of a detector based on a charge-phase qubit in a microwave field with frequency $\nu=15$ GHz with variation of the charge on the gate by the amount $\delta q \approx 0.2e$ near $n_g=0$ (Figs. 8a and 8b) and $n_g=1$ (Figs. 8c and 8d). A detailed analysis of dependences similar to those presented in Fig. 8 shows that in an electromagnetic field with generator power −60 dBm the energy level near $n_g=1\pm0.35$ depends very weakly on the change in the charge ("flat" level), and in this regime the qubit can be used as a magnetometer. The quantity $\eta_\alpha(n_g)$ increases strongly in a small neighborhood of $n_g=0\pm0.05$, and for this reason a local coefficient of transformation with respect to the charge must be introduced into the analysis. The main distinguishing feature of qubit-detectors with parametric energy transformation as a result of the periodic change of the occupation of the levels is a possible "divergence" of the coefficients of transformation as any regeneration points are approached. However, we note that the output

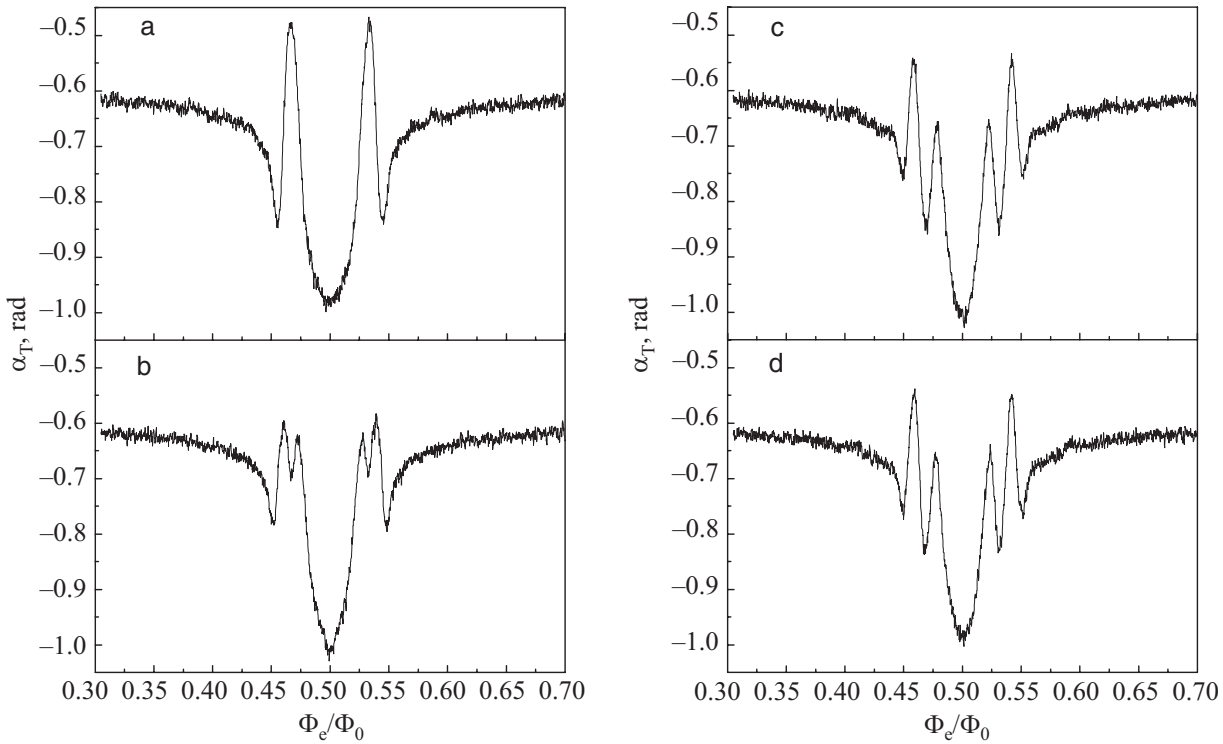

FIG. 8. Family of phase signal characteristics $\alpha_T(\Phi_e)$ charge-phase qubit in a microwave field with frequency $\nu=15$ GHz with variation of the gate charge by $\delta q \approx 0.2e$ in a neighborhood of $n_g=0$ (a, b) and $n_g=1$(c, d). The input power $P=-60$ dB for all characteristics.

fluctuations in this case likewise grow as $\eta_\alpha(n_g)$, $\eta_V(n_g)$, and $\eta_\alpha(\varphi)$, $\eta_V(\varphi)$, so that the noise at the input of the detector remains finite. In our experiments the sensitivity of a detector is determined by the effective noise temperature of the resonant circuit $T_{T*} \approx (500 \pm 100)$ mK and the inhering noise of a charge-phase qubit.

V. CONCLUSION

A classical analog of the quantum coherent effect examined above is the single-frequency nondegenerate energy input effect, studied in Ref. 42 and 43. This effect can be observed in reactive components with variable parameters only if the reactive parameter assumes negative values during a part of the period. For example, in the classical case the sign of the inductance of a Josephson junction $L_J = \Phi_0/2\pi I_C \cos\varphi$ changes periodically with frequency $\omega = 2eV/\hbar$ close to the resonance frequency of a microwave generator. In a quantum detector the effective inductance, proportional to the local curvature of the ground and excited levels (7) likewise changes sign, during a period of the low-frequency (Rabi-type) oscillations, with frequency close that of the resonant circuit. In both effects the average value of the energy exchange depends on the phase difference between two oscillators; for some value energy is transferred from the external source to the resonator $\mathrm{Re}\, Z(\omega) < 0$ while in "antiphase" energy is transferred in the opposite direction. In a qubit the sign of the average energy flux resulting in "emission" and "absorption" effects is controlled by detuning the frequency ν of the microwave radiation relative to the characteristic frequency of the qubit $(\tilde{E}_1 - \tilde{E}_0)/h$.

As follows from the results obtained (Figs. 4–8), the parametric energy transfer occurring between a qubit and a resonant circuit near $\Omega_R \cong \omega_T$ results in a sharp increase of the coefficients of transformation of a qubit-detector with respect to both the magnetic flux and charge. The main distinguishing feature of such detectors is the possibility of obtaining very large ($\sim 10^{12}$ s^{-1}) transformation coefficients (formally, the coefficients $\eta_V(\varphi)$, $\eta_\alpha(\varphi)$, $\eta_V(n_g)$, and $\eta_\alpha(n_g)$ can diverge as the oscillation band decreases). Since the contribution of the noise of the amplifying channel is proportional to η^{-2}, the noise can be neglected for large values of the transformation coefficients. In this case the noises of the resonant circuit which are due to the thermodynamic fluctuations $k_B T_{T*}$ will prevent attaining values of the sensitivity which are close to the quantum limit $\delta\varepsilon\,\delta t \approx \hbar/2$. To decrease T_{T*} and produce a fast quantum detector the pump frequency must be increased to $\Omega_P/2\pi \approx 1-2$ GHz and the measuring scheme must be modified so that the temperature of the first cascade of the cooled amplifier would be in the range 30–50 mK. Then, taking account of the back reaction of the detector on the input, the minimum sensitivity of a qubit-detector (10) based on the parametric energy transfer effect will be determined only by the inhering noise of the qubit or the quantum limit.[44]

This work was financed in part by DFG (code KR 1171/9-2) and the Ministry of Education and Science of Ukraine ("Nanophysics and nanoelectronics") M/189-07).

We wish to thank D. Born, T. Wagner, U. Hübner, I. Zhilyaev, and S. V. Kuplevakhskiĭ for fruitful discussion and helpful remarks.

[a]Email: snyrkov@ilt.kharkov.ua

[1]K. A. Valiev, Usp. Fiz. Nauk **175**, No. 1, 3 (2005).
[2]E. Schrödinger, Naturwiss. **23**, 807 (1935); *ibid* 23, 823 (1935); *ibid* 23, 844 (1935).
[3]A. J. Leggett, S. Chakravarty, A. T. Dorsey, M. P. A. Fisher, A. Garg, and W. Zwerger, Rev. Mod. Phys. **59**, 1 (1987).
[4]U. Weiss, Grabert, and S. Linkwitz, J. Low Temp. Phys. **68**, 213 (1987).
[5]Y. Nakamura, Y. A. Pashkin, and J. S. Tsai, Nature **398**, 786 (1999).
[6]J. R. Friedman, V. Patel, W. Chen, S. K. Tolpygo, and J. E. Lukens, Nature **406**, 43 (2000).
[7]Y. Makhlilin, G. Schon, and A. Shnirman, Rev. Mod. Phys. **73**, 357 (2001).
[8]G. Wendin and V. S. Shumeiko, Fiz. Nizk. Temp. **33**, 957 (2007) [Low Temp. Phys. **33**, 724 (2007)].
[9]J. Clarke and F. Wilhelm, Nature **453**, 1031 (2008).
[10]D. Vion, A. Aassime, A. Cottet, P. Joyez, C. Urbina, D. Esteve, and M. H. Devoret, Science **296**, 886 (2002).
[11]R. J. Schoelkopf, P. Wahlgren, A. A. Kozhevnikov, P. Delsing, and D. E. Proder, Science **280**, 1238 (1998).
[12]I. Chiorescu, Y. Nakamura, C. J. M. Harmans, and J. E. Mooij, Science **299**, 1869 (2003).
[13]I. Chiorescu, P. Bertet, K. Semba, Y. Nakamura, C. J. M. Harmans, and J. E. Mooij, Nature **431**, 159 (2004).
[14]A. Lupascu, S. Saito, T. Picot, P. C. De Groot, C. J. M. Harmans, and J. E. Mooij, Nat. Phys. **3**, 119 (2007).
[15]V. I. Shnyrkov, G. M. Tsoi, D. A. Konotop, and I. M. Dmitrenko, in *Proc. 4th Int. Conf. SQUID '91* (Session on SET and Mesoscopic Devices), Berlin, Germany (1991), p. 211.
[16]A. Izmalkov, M. Grajcar, E. Il'ichev, Th. Wagner, H.-G. Meyer, A. Y. Smirnov, M. H. S. Amin, A. M. van den Brink, and A. M. Zagoskin, Phys. Rev. Lett. **93**, 0370003 (2004).
[17]D. Born, V. I. Shnyrkov, W. Krech, Th. Wagner, E. Il'ichev, M. Grajcar, U. Hübner, and H.-G. Meyer, Phys. Rev. B **70**, 18051 (2004).
[18]V. I. Shnyrkov, Th. Wagner, D. Born, S. N. Shevchenko, W. Krech, A. N. Omelyanchouk, E. Il'ichev, and H.-G. Meyer, Phys. Rev. B **73**, 024506 (2006).
[19]A. N. Korotkov and D. V. Averin, Phys. Rev. B **64**, 165310 (2001).
[20]A. Yu. Smirnov, Phys. Rev. B **68**, 134514 (2003).
[21]R. Ruskov and A. N. Korotkov, Phys. Rev. B **67**, 241305 (2003).
[22]M. B. Menskiĭ, Usp. Fiz. Nauk **173**, 1199 (2003).
[23]M. Sillanpää, T. Lehtinen, A. Paila, Y. Makhlin, and P. Hakkonen, Phys. Rev. Lett. **96**, 187002 (2006).
[24]C. M. Wilson, T. Duty, F. Persson, M. Sandberg, G. Johansson, and P. Delsing, Phys. Rev. Lett. **98**, 257003 (2007).
[25]V. I. Shnyrkov and S. I. Mel'nik, Fiz. Nizk. Temp. **33**, 22 (2007) [Low Temp. Phys. **33**, 15 (2007)].
[26]A. B. Zorin, Zh. Eksp. Teor. Fiz. **125**, 1423 (2004).
[27]A. B. Zorin, Physica C **368**, 284 (2002).
[28]W. Krech, M. Grajcar, D. Born, I. Zhilyaev, Th. Wagner, E. Il'ichev, and Ya. Greenberg, Phys. Lett. A **303**, 352 (2002).
[29]I. M. Dmitreuko, G. M. Tsoi, V. I. Shnyrkov, and V. V. Kartsovnik, J. Low Temp. Phys. **49**, 417 (1982).
[30]M. T. Tuominen, J. M. Hergenrother, T. S. Tighe, and M. Tinkham, Phys. Rev. Lett. **69**, 1997 (1992).
[31]K. K. Likharev and A. B. Zorin, J. Low Temp. Phys. **59**, 347 (1985).
[32]R. Rifkin, D. A. Vincent, B. S. Deaver, and P. K. Hansma, J. Appl. Phys. **47**, 2645 (1976).
[33]V. I. Shnyrkov, V. A. Khlus, and G. M. Tsoi, J. Low Temp. Phys. **39**, 477 (1980).
[34]S. N. Shevchenko, Eur. Phys. J. B **61**, 187 (2008).
[35]M. J. Everitt, P. Stiffell, T. D. Clark, A. Vourdas, J. F. Ralph, H. Prance, and R. J. Prance, Phys. Rev. B **63**, 144530 (2001).
[36]W. Krech, D. Born, V. Shnyrkov, Th. Wagner, M. Grajcar, E. Il'ichev, H.-G. Meyer, and Y. Greenberg, IEEE Trans. Appl. Supercond. **15**(2), 876 (2009).
[37]V. I. Shnyrkov, D. Born, A. A. Soroka, and W. Krech, Phys. Rev. B **79**, 184522 (2009).
[38]O. Astafiev, Yu. A. Pashkin, Y. Nakamura, T. Yamamoto, and J. S. Tsai,

Phys. Rev. Lett. **93**, 267007 (2006).
[39]O. Astafiev, Yu. A. Pashkin, Y. Nakamura, T. Yamamoto, and J. S. Tsai, Phys. Rev. Lett. **96**, 137001 (2006).
[40]V. V. Danilov and K. K. Likharev, Radiotekh. i Élektronika **25**, 1725 (1980).
[41]M. Grajcar, A. Izmalkov, E. Il'ichev *et al.*, Phys. Rev. B **69**, 060501 (2004).
[42]H. Kanter and F. L. Vernon, Jr., J. Appl. Phys. **43**(7), 3174 (1972).
[43]A. N. Vystavkin, V. N. Gubankov, L. S. Kuz'min, K. K. Likharev, V. V. Migulin, and A. M. Spitsyn, Pis'ma Zh. Eksp. Teor. Fiz. **17**, 284 (1973) [Sov. Phys. JETP **xxx**].
[44]Yu. I. Vorontsov and F. Ya. Khalili, Radiotekh. i Élektronika **27**, 2392 (1982).

Translated by M. E. Alferieff